Configuration, stereodynamics and crystal structure of 3-substituted-2-oxofuro[2,3-*b*]indoles

Martha S. Morales-Ríos, Oscar R. Suárez-Castillo and Pedro Joseph-Nathan

Departamento de Química, Centro de Investigación y de Estudios Avanzados del Instituto Politécnico Nacional, Apartado 14-740 México, D. F. 07000, México

Received (in Cambridge, UK) 8th October 1999, Accepted 25th January 2000

The molecular structure of 3a-alkyl-3-cyano-2-oxofuro[2,3-*b*]indoles **1a**–**d** and 3a-alkyl-3-methoxycarbonyl-2-oxofuro[2,3-*b*]indoles **2a**–**c** has been determined by ^{1}H NMR spectroscopy, X-ray diffraction and semiempirical (AM1) and *ab initio* (HF/3-21G* level) quantum chemical calculations. Considering detailed NOE measurements and the anisotropic effects of the C(3) carbonyl ester group, the preferred configurations were determined in solution. In these compounds the thermodynamic preference of the C(3) electron-attracting substituent for the *endo* or *exo* face appears to be controlled by the steric demand of the C(3a) alkyl substituent. The structurally folded furoindoles *endo*-**2a**–**c** evidence a repulsive interaction between the sterically crowding CO_2Me group and the π system of the benzene ring. An increase in the solvent polarity significantly alters the *endo*:*exo* ratio in favor of the *endo* isomer. The solid-state structures of **1d** and **2a** demonstrate that these compounds assume configurations which differ in the spacial orientation of the C(3) substituent, with the CN group in **1d** oriented to the *endo* face and the CO_2Me group in **2a** to the *exo* face of the molecule, in agreement with those configurations determined in CD_2Cl_2 solution and from theoretical calculations.

Introduction

3a-Alkyl-2-oxofuro[2,3-*b*]indoles are an important class of compounds because they may easily be transformed into the corresponding fused furans, lactams, pyrroles, *etc*. These compounds are useful intermediates for the synthesis of biologically active natural products,[1] which have been isolated from diverse origins such as the *Physostigma* and *Flustra* alkaloids.[2] Configurational studies in pyrrolo[2,3-*b*]indoles and furo[2,3-*b*]-benzofurans based on NMR studies, X-ray diffraction analyses and semiempirical calculations demonstrated that, under equilibration conditions, C(2) substituents prefer to occupy the *endo* face.[3] It is proposed that differences in the minimum energy conformation [3a] are responsible for the observed favored C(2) *endo* isomer over the *exo* isomer. In contrast, with regard to the 3-substituted 2-oxofuro[2,3-*b*]indolyl system, it was presumed that the 3-substituted *exo* isomer is thermodynamically more stable than the corresponding *endo* isomer.[4]

During the course of our studies toward the synthesis of indole alkaloids, preliminary investigations [5,6] about the configuration of 3a-alkyl-3-cyano-2-oxofuro[2,3-*b*]indoles **1a**–**d** demonstrated that compounds **1a**–**c** exist as diastereoisomeric mixtures in solution and undergo fast H-3 deuterium exchange with D_2O, thus highlighting the possibility of its equilibration under neutral conditions. In contrast, although H-3 in **1d** slowly exchanges with D_2O, a single diastereoisomer is present in solution. In order to gain information concerning the combined influence of the stereoelectronic effects of the C(3) substituent and the bulkiness of the C(3a) alkyl group on the dynamic stereochemistry of these 2-oxofuro[2,3-*b*]indoles, we present herein a study of two series of 3-substituted 3a-alkyl-2-oxofuro[2,3-*b*]indoles **1a**–**d** and **2a**–**c**. In both series, we also explore the solvent effect on the thermodynamic *endo* or *exo*-face preference of the C(3) electron-attracting substituent (CN, CO_2Me). The results obtained in CD_2Cl_2 solution were compared with calculations performed at the semiempirical and *ab initio* levels. In addition, X-ray diffraction studies were performed on single crystals of **1d** and **2a** in order to explore further the stereochemical preference of these compounds in the solid state.

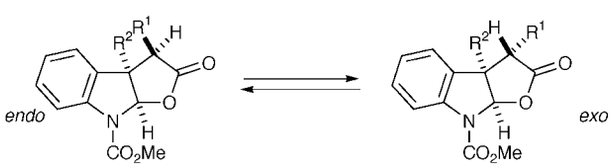

1a-d
2a-c

1a-c
2a-c

	R^1	R^2			
		a	**b**	**c**	**d**
1	CN	Me	Et	Pr^i	Bu^t
2	CO_2Me	Me	Et	Pr^i	–

Results and discussion

NMR spectra

The new 3-methoxycarbonyl-2-oxofuro[2,3-*b*]indoles **2a**–**c** were prepared by rearrangement, in basic media, of the corresponding 3-cyano-2-oxofuro[2,3-*b*]indoles **1a**–**c** followed by acid-catalysed hydrolysis [7] of the resulting 2-amino-3-methoxycarbonylfuro[2,3-*b*]indoles **3a**–**c** in 65–68% overall yield (Scheme 1). As in the case of furoindoles **1a**–**c**,[6] in solution furoindoles **2a**–**c** also proved to be mixtures of *endo*/*exo* epimers. The detailed NMR assignments were based on integration,

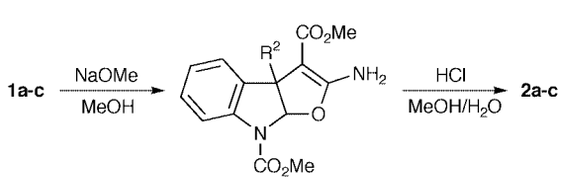

3a-c

Scheme 1

DOI: 10.1039/a908104f

^{1}H–^{1}H coupling constants and 2-D experiments. The ^{1}H NMR spectral data of **1a**–**d** and **2a**–**c**, obtained in $(CD_3)_2SO$ and in CD_2Cl_2 solutions, are reported in Table 1. The configuration for both series of compounds **1a**–**d** and **2a**–**c** was determined by NOE ^{1}H NMR experiments upon irradiation of the angular C(3a) alkyl group as summarized in Table 2 and confirmed, in the case of **2a**–**c**, by the diamagnetic anisotropy effect exerted by the carbonyl ester group.

The ^{1}H NMR spectra of 3-substituted furoindoles **1a**–**c** and **2b**,**c**, measured in CD_2Cl_2 solution at room temperature, exhibit two sets of signals of different intensity, while for **1d** and **2a**, even in a low-noise ^{1}H NMR spectrum, only one set of signals was detected. In all cases, the signals are sharp excepting those owing to the angular proton H-8a, H-7 and the methyl carbamate protons. In $(CD_3)_2SO$ solution, only **1d** appears as a single epimer. In this solvent the H-8a signal for the *endo* and *exo* isomers is sharp, whereas those owing to H-7 and the methyl protons of the carbamate group remain broad. The broadness of these signals suggests the presence of conformational isomers arising from slow rotation around the N–CO_2Me bond.[8] Of additional interest is that the chemical shift of the proton (H-3) bonded to the carbon at which CN or CO_2Me group is attached exhibits a strong solvent dependence. For example, the shift of H-3 for *exo*-**1a** is seen at δ 4.10 in CD_2Cl_2 and δ 5.07 in $(CD_3)_2SO$, whereas H-3 for *exo*-**2a** is seen at δ 3.90 in CD_2Cl_2 and δ 4.28 in $(CD_3)_2SO$, indicating hydrogen bonding associations involving the H-3 and the DMSO solvent. Within this context, the larger acceptor power of CN with respect to CO_2Me is also evident. The attribution of the aromatic protons was obtained from *J*(HH) values and homonuclear irradiation experiments.

Conformation and stereodynamics of the furoindoles 1a–d and 2a–c

Strong experimental support for the stereochemical preference of the furoindoles **1** and **2** comes from steady-state, difference NOE measurements and from the chemical shift of the H-4 proton signal obtained in DMSO-d_6 and CD_2Cl_2 solutions. For example, although irradiation of the closely spaced C(3a) methyl signals (Table 2) of the *endo*/*exo* mixture in **1a** was not selective in $(CD_3)_2SO$, the conclusion is clear and resulted in positive NOEs (17 and 22%) for the signals at δ 5.11 and 6.44 due to H-3 and H-8a of the major epimer, as well as a positive NOE (21%) for the signal at δ 6.54 due to H-8a, respectively, of the minor epimer. In the case of **2a**, selective irradiation of the signal at δ 1.61 due to the C(3a) methyl group of the major epimer resulted in a large enhancement (21%) of the signal at δ 4.35 due to H-3 and also a large enhancement (19%) of the signal at δ 6.28 due to the H-8a proton. The obtained results unambiguously revealed that, for the major epimers, the CN and CO_2Me groups are arranged in an *anti* relationship with respect to the C(3a) alkyl group, and therefore the *endo* stereochemistry in series **1** and **2** is thermodynamically preferred over the *exo* stereochemistry, in the polar DMSO solvent. The NOE experiments in methylene chloride (Table 2) allowed also unequivocal *endo*/*exo* assignment. For *endo* epimers NOEs of 17–27% were observed for the H-3 and H-8a protons, upon irradiation at the C(3a) methyl protons of the alkyl group of the major epimer in **1a** and **1d**, whereas a NOE was not detected for H-3 when the methyl protons of the minor *exo*-**1a** epimer were irradiated.

As another independent criterion for the *endo*/*exo* stereochemical assignment of compounds **2a**–**c** in DMSO, the significant differences in their ^{1}H NMR chemical shifts were considered (Table 1). Thus, the signal for H-4 of the major isomer was shifted *ca*. 0.50 ppm to high field relative to the minor isomer, while the other peaks exhibited no appreciable change, indicating that H-4 lays well in the shielding current of the carbonyl ester group. In addition, the methyl, methylene or

Table 1 ^{1}H NMR chemical shifts (δ) of furoindoles **1a**–**d** and **2a**–**c** (in DMSO-d_6 and in CD_2Cl_2)

Compound	H-3 (s)	H-4 (dd)	H-5 (td)	H-6 (td)	H-7 (br, s)	H-8a (s)	R^1 (s)	R^2	NCO_2CH_3 (s)
endo-**1a**	5.11; *4.13*	7.59; *7.64*	7.23; *7.21*	7.43; *7.41*	7.75; *7.80*	6.44; *6.28*	—	1.57; *1.65* (s, CH_3)	3.87; *3.91*
exo-**1a**	5.07; *4.10*	7.52; *7.26*	7.17; *7.18*	7.37; *7.38*	7.75; *7.80*	6.54; *6.29*	—	1.63; *1.71* (s, CH_3)	3.87; *3.91*
endo-**1b**	5.19; *4.17*	7.57; *7.63*	7.23; *7.22*	7.45; *7.43*	7.73; *7.86*	6.46; *6.30*	—	2.02, 1.97; *2.05*, *1.96* (2dq, CH_2), 0.73; *0.89* (t, CH_3)	3.86; *3.92*
exo-**1b**	5.11; *4.11*	7.48; *7.24*	7.16; *7.18*	7.38; *7.39*	7.73; *7.86*	6.63; *6.34*	—	2.11, 2.05; *2.17*, *2.13* (2dq, CH_2), 0.67; *0.85* (t, CH_3)	3.86; *3.92*
endo-**1c**	5.25; *4.19*	7.59; *7.67*	7.24; *7.22*	7.47; *7.44*	7.76; *7.89*	6.47; *6.29*	—	2.41; *2.21* (h, CH), 1.06, 0.53; *1.13*, *0.77* (2d, 2 CH_3)	3.87; *3.92*
exo-**1c**	5.22; *4.08*	7.59; *7.24*	7.19; *7.17*	7.42; *7.41*	7.76; *7.89*	6.80; *6.38*	—	2.60; *2.61* (h, CH), 1.00, 0.55; *1.12*, *0.72* (2d, 2 CH_3)	3.87; *3.92*
endo-**1d**	5.37; *4.35*	7.70; *7.77*	7.26; *7.22*	7.50; *7.44*	7.78; *7.90*	6.50; *6.40*	—	0.97; *1.05* (s, $C(CH_3)_3$)	3.89; *3.92*
endo-**2a**	4.35; *a*	6.98; *a*	7.10; *a*	7.35; *a*	7.71; *a*	6.28; *a*	3.67; *a*	1.61; *a* (s, CH_3)	3.86; *a*
exo-**2a**	4.28; *3.90*	7.53; *7.27*	7.17; *7.15*	7.38; *7.34*	7.71; *7.84*	6.38; *6.28*	3.84; *3.86*	1.33; *1.39* (s, CH_3)	3.88; *3.92*
endo-**2b**	4.34; *3.91*	6.96; *6.96*	7.12; *7.08*	7.37; *7.33*	7.73; *7.84*	6.33; *6.21*	3.63; *3.60*	2.11, 2.04; *2.12*, *2.02* (2dq, CH_2), 0.65; *0.82* (t, CH_3)	3.87; *3.92*
exo-**2b**	4.31; *3.91*	7.53; *7.26*	7.19; *7.16*	7.40; *7.36*	7.73; *7.84*	6.43; *6.33*	3.83; *3.85*	1.79, 1.67; *1.89*, *1.71* (2dq, CH_2), 0.62; *0.71* (t, CH_3)	3.88; *3.92*
endo-**2c**	4.40; *4.01*	7.00; *6.99*	7.12; *7.08*	7.38; *7.34*	7.75; *7.86*	6.31; *6.21*	3.56; *3.86*	2.42; *2.29* (h, CH), 0.95, 0.70; *0.96*, *0.93* (2d, 2 CH_3)	3.88; *3.92*
exo-**2c**	4.39; *3.96*	7.57; *7.25*	7.20; *7.15*	7.43; *7.38*	7.75; *7.86*	6.48; *6.39*	3.85; *3.86*	2.20; *2.27* (h, CH), 0.90, 0.47; *1.00*, *0.56* (2d, 2 CH_3)	3.90; *3.92*

a Not detected.

Table 2 Quantitative NOEs (%) for selected furoindoles **1a**, **1d**, **2a** and **2b** measured at 300 MHz in DMSO-d_6 and/or CD_2Cl_2 solvents at 25 °C

		Observed proton					
	Irradiated protons	DMSO-d_6			CD_2Cl_2		
Compound	C(3a)R^2	H-3	H-4	H-8a	H-3	H-4	H-8a
endo-**1a**	CH_3	17	10	22	24	8	17
exo-**1a**	CH_3	N.d.	N.d.	21	N.d.	5	16
endo-**1d**	*tert*-Bu				27	19	26
endo-**2a**	CH_3	21	13	19			
exo-**2a**	CH_3	N.d.	5	20			
endo-**2d**	CH_2				10	5	3
exo-**2b**	CH_2				N.d.	N.d.	7

N.d. = not determined.

Table 3 Solvent effects over the *endo*:*exo* ratio[a] and free energy differences $\Delta G°$[b] of furoindoles **1a**–**d** and **2a**–**c**

		endo:*exo*					
Entry	Compound	DMSO-d_6	MeOD-d_3	Acetone-d_6	$CDCl_3$	CD_2Cl_2	$\Delta G°$[c]/kJ mol^{-1}
1	**1a**	1:0.25	1:0.30	1:0.30	1:0.45	1:0.45	2.00
2	**1b**	1:0.15	1:0.15	1:0.15	1:0.40	1:0.30	2.98
3	**1c**	1:0.10	1:0.15	1:0.15	1:0.25	1:0.20	4.00
4	**1d**	≥1:0.02	≥1:0.02	≥1:0.02	≥1:0.02	≥1:0.02	≥9.7
5	**2a**	1:0.80	1:1.30	1:2.00	1:9.00	≥1:50	≥9.7
6	**2b**	1:0.60	1:0.80	1:1.20	1:1.20	1:1.50	1.00
7	**2c**	1:0.50	1:0.80	1:1.10	1:1.00	1:1.20	0.45

[a] Determined by ^{1}H NMR integration of H-8a and/or H-3. [b] $\Delta G°$ Estimated by $-RT \ln K$ (at 25 °C, in CD_2Cl_2). [c] K = [major isomer]/[minor isomer].

methine signals of the corresponding C(3a) alkyl group (R^2) of the minor isomers were shifted *ca*. 0.25 ppm to high field relative to the signals of the major isomer. These results further confirm the *anti* relationship between the CO_2Me group and the C(3a) alkyl group in major furoindoles **2a**–**c**.

Another important aspect derived from the diamagnetic anisotropy effect exerted by the carbonyl ester group was the opportunity to determine spatial relationships and thereby to establish the preferred conformation of the isomeric furoindoles **2a**–**c**. The H-4 signal for the *exo* epimers occur at a rather expected δ 7.50 in $(CD_3)_2SO$ by analogy with **1a**–**d**, while H-4 for the *endo* epimers is shielded at δ 7.00. These shifts correspond to having the H-4 for the *endo* epimers in the shielding current of the carbonyl ester group, thus identifying the rotamer in which the C=O ester group is *anti* with respect to the C2–C3 bond of the lactone ring. Analysis of ^{1}H NMR data for the corresponding C(3a) alkyl group in the *exo* isomers also argues in favor of an *anti* relationship between the C=O ester group and the C2–C3 bond. Dipole–dipole interactions[9] between the C=O ester and the C=O lactone groups play an important role in determining the conformational preference. Crystallographic data of **1d** (R^1 = CN, R^2 = *tert*-Bu) and **2a** (R^1 = CO_2Me, R^2 = Me) and quantum chemical calculations (*vide infra*) are both in agreement with solution results.

Solvent effects on the configuration of the furoindoles 1a–d and 2a–c

The ^{1}H NMR measurements of samples of compounds **1a**–**d** and **2a**–**c** (0.07 M) in solvents of different polarities ($(CD_3)_2SO$, CD_3OD, $(CD_3)_2CO$, $CDCl_3$, CD_2Cl_2) at room temperature indicated that the *endo*:*exo* ratio of these compounds exhibited a pronounced solvent dependence. The solvent effect on the equilibrium ratio and the free energy difference $\Delta G°$ of the *endo*/*exo* epimers in CD_2Cl_2 solution, calculated by solving the Eyring equation, are reported in Table 3. Inspection of Table 3 shows the following trends. (i) As the angular C(3a) alkyl substituent becomes bulkier, the *endo* epimer increases. (ii) In all cases, with the exception of **1d** (in all solvents used, entry 4) and **2a** (in CD_2Cl_2, entry 5), an equilibrated mixture of *endo*/*exo* epimers is present. Of course, the increased strain by the sterically bulkier *tert*-butyl group in **1d** favored the thermodynamically more stable *endo*-configurated isomer. Since the *exo* epimer for **1d** and the *endo* epimer for **2a** (in CD_2Cl_2) were not detected in a low-noise ^{1}H NMR spectrum, the *endo*:*exo* ratio was estimated to be ≥50:1 and ≥1:50, respectively. (iii) Independently of the solvent used, when the CN group is replaced by the CO_2Me group, the *endo*:*exo* ratio is improved in favor of the *exo* epimer. However, the *endo* epimers prevail in DMSO (entries 5–7). This is likely because of the increased steric crowding of the CO_2Me group *versus* the CN group, in conjunction with the destabilizing van der Waals overlap of the carbonyl ester group and the H-4 proton of the benzene ring. (iv) The solvent change from DMSO to the less polar methylene chloride also significantly alters the *endo*:*exo* ratio in favor of the *exo* epimer. The most dramatic example is seen in **2a** for which the *endo*:*exo* ratio varies from 1:0.80 in DMSO to an estimated factor of ≥1:50 in methylene chloride (entry 5). The solvent-dependent *endo*:*exo* ratio can be attributed to differential solvation, where polar solvents preferentially solvate the more polar epimer relative to the less polar epimer.[10] Additionally, differential solute–solvent hydrogen-bonding interactions, involving the acidic H-3 proton, could favor the *endo* epimer.

Quantum chemical calculations

In order to find whether a possible correlation could be established between the stereochemical *endo*/*exo* preference of furoindoles **1** and **2** determined experimentally (NMR) and their relative stabilities, the estimation of the total energies for the model compounds **1a** (R^1 = CN, R^2 = Me) and **2a** (R^1 = CO_2-Me, R^2 = Me) was carried out. Concerning the furoindole **1a**, *ab initio* calculations performed at the HF/3-21G* level predict that the most stable structure corresponds to the *endo* epimer with a relative energy difference (E_{rel}) between the *endo* and *exo* epimers of 2.1 kJ mol^{-1}. The computational *endo* and *exo* configurations are illustrated in Fig. 1 along with their relative energies. Furthermore, if it is assumed that the entropic and

Table 4 Theoretical energies, relative energies and dihedral angles (C2–C3–C9–O9) for the conformational minima of *endo*- and *exo*-furoindoles **2a**

		AM1			HF/3-21G*		
Compound	Conformer[a]	ΔH_f/ kJ mol^{-1}	E_{rel}/ kJ mol^{-1}	Dihedral angle/° C2–C3–C9–O9	*E*/hartree	E_{rel}/ kJ mol^{-1}	Dihedral angle/° C2–C3–C9–O9
endo-**2a**	*anti*	−794.73	7.2	157.6	−1074.433 770	14.3	148.5
	syn	−791.90	9.7	−22.5	−1074.433 278	15.6	−9.4
exo-**2a**	*anti*	−801.50	0.1	−146.8	−1074.439 217	00	−127.4
	syn	−801.62	0	53.2	−1074.436 779	06.4	69.5

[a] See Fig. 2.

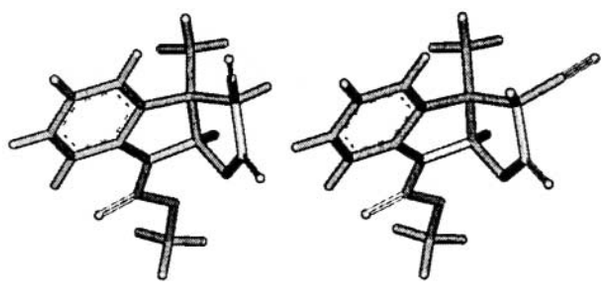

endo-**1a** *exo*-**1a**

E = -940.272989 hartree
E_{rel} = 0 kJ mol^{-1}

E = -940.272177 hartree
E_{rel} = 2.132 kJ mol^{-1}

Fig. 1 Optimized geometries, calculated energies (*E*/hartree) and relative energy difference (E_{rel}/kJ mol^{-1}) for *endo*-**1a** and *exo*-**1a** obtained at the *ab initio* (HF/3-21G*) level.

solvation contributions are not important in the equilibrium between these epimers, the calculated difference in free energy (2.1 kJ mol^{-1}) means a value of 2.4 for the corresponding equilibrium constant, consistent with the $\Delta G°$ value derived from the observed *endo*/*exo* populations in the NMR spectra measured in CD_2Cl_2 solvent (Table 3).

In the case of compound **2a**, in order to insure that the relative energy value of the global minimum has been considered to predict the relative stabilities of the *endo* and *exo* epimers, its conformational profiles were studied. The calculations were performed at the semiempirical level (AM1) and the minima points of the resulting energetic profile for the rotation about the C3–C9 bond were further optimized at the level of *ab initio* quantum chemistry (HF/3-21G*). The changes in the total energy with the dihedral angle between C2–C3–C9–O9 of the *endo* and *exo* epimers **2a** were calculated by a stepwise variation of the dihedral angle in 10° increments. The calculations gave two conformational barriers for each epimer, in which the most important is generated by the close interaction of the carbonyl groups,[9] and two ground state conformations corresponding to the rotamers with the C=O ester group *syn* or *anti* to the C2–C3 bond of the lactone ring. These 4 conformations for the *endo* and *exo* epimers are illustrated in Fig. 2. As shown the two ground state conformations for *endo*- and *exo*-**2a** can be converted into each other by overcoming energy barriers of 15.7 and 9.5 kJ mol^{-1}, respectively.

The comparison of the relative energy values of the minima for *endo*-**2a** calculated by the AM1 method indicated that the absolute minimum corresponds to the *anti* rotamer by only 2.5 kJ mol^{-1}, while *ab initio* calculations indicate that both conformations are almost isoenergetic. In Table 4 are summarized the energies of the ground state conformers for the two methods used (semiempirical and *ab initio*) together with the corresponding dihedral angles C2–C3–C9–O9. For the *exo*-**2a** epimer, semiempirical calculations predict that the two ground state conformations (*anti* and *syn*) are essentially isoenergetic, whereas *ab initio* calculations indicate that the *anti* conformer is more stable than the *syn* conformer by 6.4 kJ mol^{-1}. It is interesting that, independently of the method used, the *exo* configuration in **2a** is found to be more stable than the *endo* configuration. The *ab initio* calculations predict that the *exo* epimer in the *anti* conformation is strongly preferred over the corresponding *endo* epimer by a ratio of 320 : 1, and with a relative energy difference of 14.3 kJ mol^{-1}. The $\Delta G°$ value derived from the observed *endo*/*exo* populations in the ^{1}H NMR spectra, measured in CD_2Cl_2 solvent, was entirely consistent with the above observations (Table 3). The predicted preferred *anti* conformation for *endo*- and *exo*-**2a** matches very well with the inferred C=O ester group orientation from the NMR spectra. In particular, for *endo*-**2a** in the *anti* conformation, the repulsive interaction between the C=O ester group and the π system of the benzene ring, the Coulombic dicarbonylic repulsion, and the van der Waals overlap of the C=O ester group and the H-4 proton of the aromatic ring are minimized.

X-Ray crystallographic analyses of compounds 1d and 2a

As has been previously reported, it is not unusual for observed solid state conformations to differ from those determined in solution and by theoretical calculations.[11] It is therefore useful directly to compare the calculated parameters with the conformational and configurational preferences observed in the crystalline state of compounds **1d** and **2a**. The molecular structures and the adopted atom numbering are presented in Fig. 3. Relevant angles and dihedral angles are listed in Table 5. In general, the optimized structures of **1d** and **2a** agree very well with the corresponding crystal structures.

As is evident from the drawings, the crystal structures of **1d** and **2a** are characterized by a folded shape along the C3a–C8a bond. The folding angles θ_1 and θ_2, formed by atoms C3b–C3a–C3 and N8–C8a-O1, for **1d** are very similar to those of **2a** (θ_6, θ_7). The structures show a *cis*-like fusion of the two five-membered rings (φ_1 and φ_5, respectively). These rings adopt an envelope conformation in which C-8a for the B ring and C-3a for the C ring are the flaps. In **1d** the *tert*-Bu and the CN groups are arranged in an *anti* relationship with each other (φ_2 and φ_3), in sharp contrast with that of the 3-methoxycarbonyl derivative **2a**, in which the Me and the CO_2Me groups are arranged in a *syn* orientation (φ_6 and φ_7), in spite of the extended steric hindrance in **2a** due to the more voluminous CO_2Me with respect to CN. In addition, the dihedral angles φ_8 (112.5°) and φ_9 (−134.0°) about the bond between the carbonyl ester group and the C ring clearly indicate the *anti* conformation between the C=O ester group and the C2–C3 bond of the lactam ring. This means that the protons of the C(3a) Me group come close to the shielding current of the C=O group, in agreement with the NMR results and theoretical predictions. As expected, the CO_2Me groups in **1d** and **2a** are in the more stable *Z* conformation, with the *O*-methyl group eclipsing the carbonyl group.[12] The nitrogen atom in **1d** and **2a** is trigonal planar as the sum of the bond angles around N8 is 360.0 (θ_3, θ_4 and θ_5) and 358.9° (θ_8, θ_9 and θ_{10}), respectively. In this planar conformation, delocalization of electrons from the nitrogen to the carbonyl group increases the N–C bond order, consistent with the

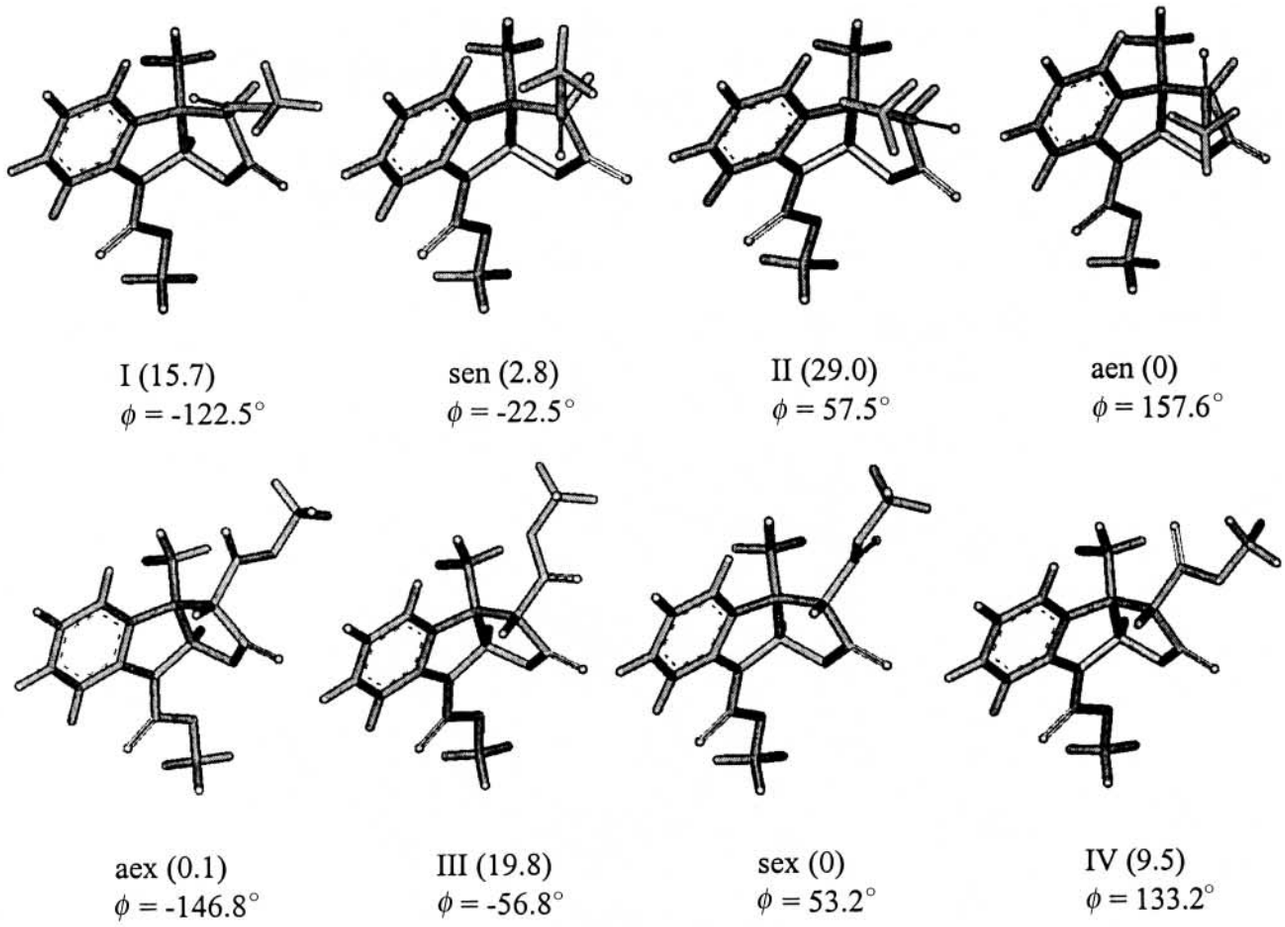

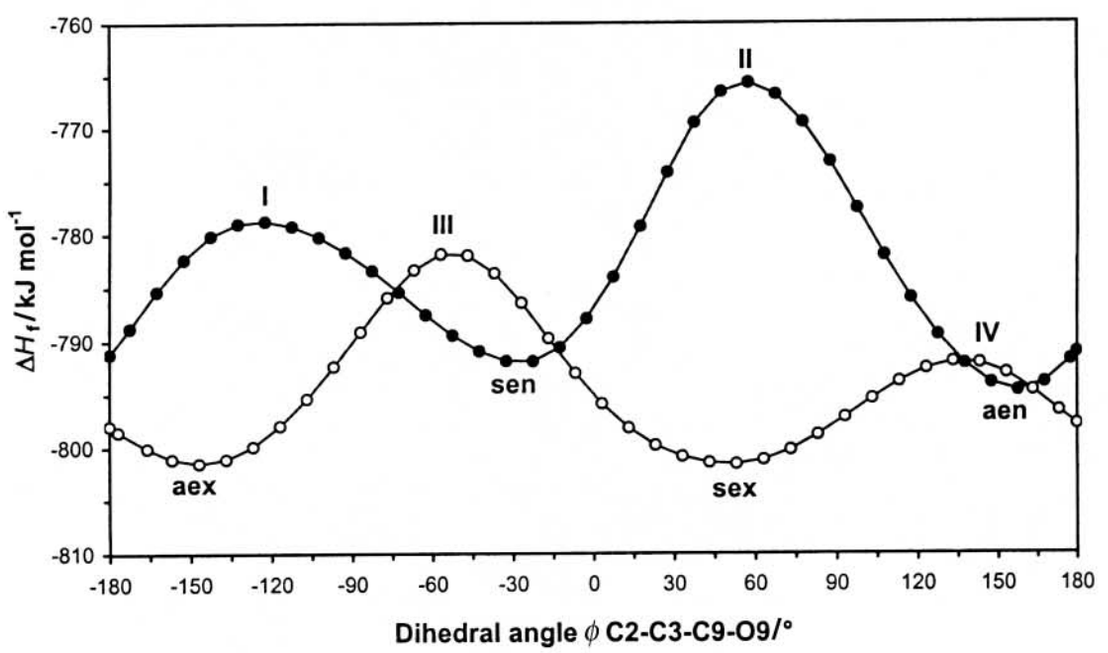

Fig. 2 Conformational profiles of *endo*-**2a** (–●–●–) and *exo*-**2a** (–○–○–) obtained at the semiempirical (AM1) level. The minima points in each case were optimized at the *ab initio* (HF/3-21G*) level, and the corresponding two stable conformers for *endo*-**2a** and *exo*-**2a** are also depicted. Relative energy (kJ mol^{-1}) in parentheses. The ϕ dihedral angle is defined by C2–C3–C9–O9. Stereochemical designation for the stable conformers: *anti-endo* (**aen**), *syn-endo* (**sen**), *anti-exo* (**aex**) and *syn-exo* (**sex**).

observed restricted rotation of this carbamate bond in the NMR spectra. Structures **1d** and **2a** show an *E* geometry about the carbamate bond (N8–C14), with the carbonyl group oriented *syn* to the aromatic ring (φ_4 and φ_{10}).

Conclusions

A full configurational and conformational analysis of 3a-alkyl-2-oxofuro[2,3-*b*]indoles **1a**–**d** and **2a**–**c** has been carried out on

Table 5 Relevant angles (θ) and dihedral angles (φ) of compounds **1d** and **2a**

Compound	Bond angle	Atoms		Dihedral angle	Atoms	
1d	θ_1	C3b–C3a–C3	113.6°	φ_1	C10–C3a–C8a–H8	−21.2°
1d	θ_2	N8–C8a–O1	107.6°	φ_2	C9–C3–C3a–C10	−93.7°
1d	θ_3	C14–N8–C7a	126.1°	φ_3	H3–C3–C3a–C10	20.5°
1d	θ_4	C14–N8–C8a	124.5°	φ_4	O14–C14–N8–C7a	2.7°
1d	θ_5	C7a–N8–C8a	109.4°			
2a	θ_6	C3b–C3a–C3	113.3°	φ_5	C10–C3a–C8a–H8	25.6°
2a	θ_7	N8–C8a–O1	107.8°	φ_6	C9–C3–C3a–C10	−31.8°
2a	θ_8	C14–N8–C7a	126.1°	φ_7	H3–C3–C3a–C10	88.4°
2a	θ_9	C14–N8–C8a	123.1°	φ_8	C3a–C3–C9–O9	112.5°
2a	θ_{10}	C7a–N8–C8a	109.8°	φ_9	C2–C3–C9–O9	−134.0°
2a				φ_{10}	O14–C14–N8–C7a	3.7°

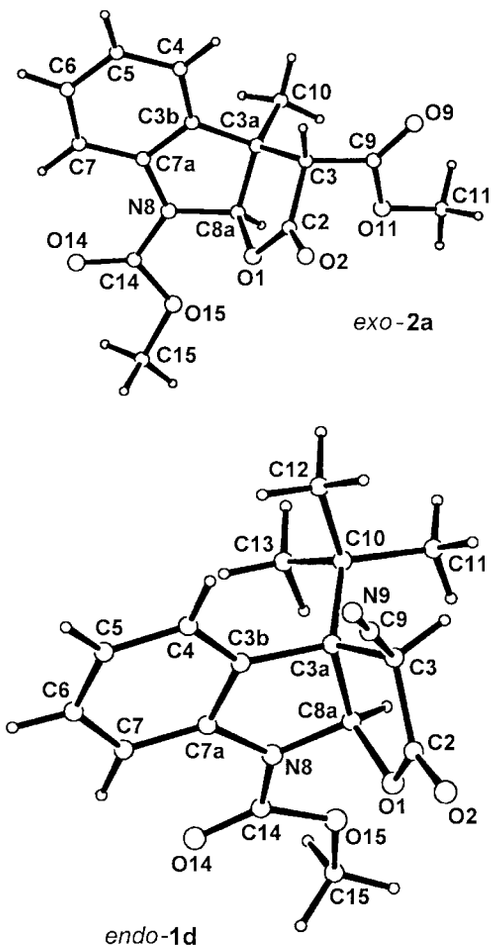

Fig. 3 Crystal structures and atom numbering for compounds *endo*-**1d** and *exo*-**2a**.

the basis of experimental NMR data, the results of X-ray analyses and calculations. The configurational preference is determined by the bulkiness of the angular C(3a) alkyl substituent, the C(3) functional group and the solvent polarity. The furoindoles show different preferred conformations in CD_2Cl_2 solution. The quantum chemical *ab initio* (HF/3-21G*) calculations of **1a** and **2a** were entirely consistent with the above observations, indicating that the *endo*-**1a** epimer is more stable than the corresponding *exo* epimer, in contrast to that predicted for **2a** in which the *exo* epimer is the preferred one. The predicted most stable *exo* configuration for **2a** is also the same as that found in the solid state. The energetic profiles of the rotation of the C3–C=O bond of *endo*- and *exo*-**2a** show two minima within a small energetic range (less than 3 kJ mol^{-1}), corresponding to the rotamers with the C=O ester group *syn* or *anti* to the C2–C3 bond of the lactone ring. The *syn* conformation, with the lowest energy minimum, is in agreement with the conformation found in solution and in the crystal structure.

Experimental

General

The furoindolic β-enaminoesters **3a**–**3c** were prepared from the corresponding methyl 3,3a,8,8a-tetrahydro-3a-alkyl-3-cyano-2-oxo-2*H*-furo[2,3-*b*]indole-8-carboxylates **1a**–**1c** according to previously published procedures.[5,13] Deuteriated solvents were purchased from Aldrich. Melting points were determined on a Fisher–Johns apparatus and are uncorrected. IR spectra were obtained using a Perkin-Elmer 16F PC spectrophotometer, ^1H and ^{13}C NMR spectra on a Varian XL300GS spectrometer working at 300 and 75.4 MHz, respectively. All chemical shifts are reported in δ units relative to TMS. Multiplicities are indicated by: s (singlet), d (doublet), t (triplet), q (quartet), h (heptet), m (multiplet), br (broad). Electron impact mass spectra (EIMS) were recorded on a Hewlett Packard 5989A spectrometer. Flash column chromatography was performed with 230–400 mesh silica gel. Analytical thin-layer chromatography was performed on silica gel plates with F-254 indicator, and the visualization was accomplished by an UV lamp (254 nm).

Theoretical methods

The *endo* and *exo* structures of compound **1a** were initially built using SYBYL force field calculations,[14] submitted to the AM1 semiempirical calculation routine level[15] and optimized by *ab initio* calculations at the HF/3-21G* level of theory[16] as implemented in Spartan plus 1.5.[17] The conformational profiles of the rotation about the C3–C9 bond were generated for *endo*- and *exo*-**2a** in 10° steps and calculated at the semiempirical level of theory using the AM1 Hamiltonian. The resulting minima points were further optimized by *ab initio* (HF/3-21G*) calculations to achieve the ground state conformations. For a better view of **1a** and **2a** the coordinates of these molecules were imported into the WebLab ViewerLite 3.20 program.

Crystallography

The intensity data for compounds *endo*-**1d** and *exo*-**2a** were collected on a Nicolet P3 diffractometer interfaced to a DEC VAXstation 4000–60 operated with Crystal Logic Inc. (Los Angeles, CA, USA) software using the θ–2θ scan technique with scan limits $3 \leq 2\theta \leq 110°$. The structures were solved by the direct methods program SHELX 86.[18] Full-matrix least-squares refinement of atomic positional and thermal parameters was performed anisotropically for non-hydrogen atoms and isotropically for hydrogen atoms. Crystal data are given in Table 6.

CCDC reference number 188/222.

Table 6 Crystal data and experimental conditions for compounds **1d** and **2a**

	1d	**2a**
Chemical formula	$C_{17}H_{18}N_2O_4$	$C_{15}H_{15}NO_6$
Molecular weight	314.3	305.3
Crystal system	Triclinic	Monoclinic
Space group	$P\bar{1}$	$P2_1/c$
Z	2	4
a/Å	7.538(1)	8.776(2)
b/Å	8.737(1)	14.019(3)
c/Å	14.100(1)	11.740(2)
α/°	90.659(4)	—
β/°	69.854(3)	95.138(9)
γ/°	110.492(4)	—
V/Å^3	810.21	1438.48
μ(Cu-Kα)/cm^{-1}	7.27	8.89
T/K	298	298
Reflections measured	2270	2093
Independent reflections	2032 (R(int) = 0.022)	1808 (R(int) = 0.069)
$R(F)$ (%)	5.5	5.1
$R(W)$ (%)	7.0	6.0

Synthesis

***cis*-(±)-Dimethyl 3a-alkyl-2-oxo-3,3a,8,8a-tetrahydro-2*H*-furo[2,3-*b*]indole-3,8-dicarboxylates 2a–2c: general procedure.** To a solution of the appropriate furoindolic β-enaminoester **3a**–**3c** (0.35 mmol) in methanol (5 mL), 1 M HCl (0.5 mL) was added and the reaction mixture stirred for 6 h at reflux. After cooling, the reaction mixture was neutralized with 40% aqueous NaOH. The resultant solution was poured into water (40 mL) and extracted with ethyl acetate (4 × 30 mL). The combined organic layer was dried (Na_2SO_4), concentrated *in vacuo* and purified by flash column chromatography with ethyl acetate–hexane (1 : 3) as the eluent.

cis-(±)-Dimethyl 3a-methyl-2–oxo-3,3a,8,8a-tetrahydro-2*H*-furo[2,3-*b*]indole-3,8-dicarboxylate (**2a**): yield: 80.1 mg, 75%; white crystals (Et_2O); mp 155–156 °C. IR ($CHCl_3$): ν 1790 (C=O lactone), 1734 cm^{-1} (C=O ester and carbamate). ^{13}C NMR (DMSO-d_6): δ (*endo* and *exo*) 169.3 and 169.5 (s, C=O lactone), 166.4 and 166.7 (s, C=O ester), 152.2 (s, C=O carbamate), 139.5 and 138.3 (s, C-7a), 131.2 and 133.7 (s, C-3b), 129.3 and 129.6 (d, C-6), 124.2 and 124.4 (d, C-4), 123.7 and 124.4 (d, C-5), 114.6 and 114.7 (d, C-7), 95.4 and 96.3 (d, C-8a), 55.5 and 56.0 (d, C-3), 53.3 and 53.4 (q, OCH_3 carbamate), 52.2 and 53.1 (q, OCH_3 ester), 51.3 (s, C-3a), 24.8 and 20.1 (q, CH_3). MS: m/z (%) = 305 (M^+, 76), 202 (100), 158 (33).

cis-(±)-Dimethyl 3a-ethyl-2-oxo-3,3a,8,8a-tetrahydro-2*H*-furo[2,3-*b*]indole-3,8-dicarboxylate (**2b**): yield 80.5 mg, 72%; colourless oil. IR ($CHCl_3$): ν 1790 (C=O lactone), 1732 cm^{-1} (C=O ester and carbamate). ^{13}C NMR (DMSO-d_6): δ (*endo* and *exo*) 169.6 (s, C=O lactone), 166.6 and 166.8 (s, C=O ester), 152.1 (s, C=O carbamate), 140.4 and 139.4 (s, C-7a), 129.6 and 129.9 (d, C-6), 129.1 and 131.0 (s, C-3b), 124.6 and 125.3 (d, C-4), 123.8 and 124.3 (d, C-5), 114.5 and 114.7 (d, C-7), 94.0 and 95.6 (d, C-8a), 55.5 (s, C-3a), 55.0 and 56.0 (d, C-3), 53.4 and 53.5 (q, OCH_3 carbamate), 52.3 and 53.2 (q, OCH_3 ester), 30.8 and 26.0 (t, CH_2CH_3), 8.1 and 7.9 (q, CH_2CH_3). MS: m/z (%) = 319 (M^+, 70), 216 (100), 172 (26).

cis-(±)-Dimethyl 3a-isopropyl-2-oxo-3,3a,8,8a-tetrahydro-2*H*-furo[2,3-*b*]indole-3,8-dicarboxylate (**2c**): yield 81.4 mg, 70%; white solid (ethyl acetate/hexane); mp 135–137 °C. IR ($CHCl_3$): ν 1790 (C=O lactone), 1732 cm^{-1} (C=O ester and carbamate). ^{13}C NMR (DMSO-d_6): δ (*endo* and *exo*) 170.1 and 169.4 (s, C=O lactone), 167.0 and 166.7 (s, C=O ester), 152.0 (s, C=O carbamate), 140.9 and 140.0 (s, C-7a), 129.5 and 130.1 (d, C-6), 127.4 and 129.2 (s, C-3b), 125.5 and 126.8 (d, C-4), 123.3 and 123.9 (d, C-5), 114.5 (d, C-7), 94.0 and 95.8 (d, C-8a), 58.8 (s, C-3a), 54.9 and 56.2 (d, C-3), 53.4 and 53.5 (q, OCH_3 carbamate), 52.3 and 53.2 (q, OCH_3 ester), 35.00 and 30.5 (d, $CH(CH_3)_2$), 17.7, 16.6 and 17.2, 16.7 (d, $CH(CH_3)_2$). MS: m/z (%) = 333 (M^+, 99), 246 (60), 230 (100).

Acknowledgements

This work was supported in part by CONACYT (México).

References

1 M. S. Morales-Ríos, O. R. Suárez-Castillo and P. Joseph-Nathan, *J. Org. Chem.*, 1999, **64**, 1086; J. P. Marino, S. Bogdan and K. Kimura, *J. Am. Chem. Soc.*, 1992, **114**, 5566; K. Shishido, T. Azuma and M. Shibuya, *Tetrahedron Lett.*, 1990, **31**, 219; Q.-S. Yu, W.-M. Luo and Y.-Q Li, *Heterocycles*, 1993, **36**, 1279; S. Horne, N. Taylor, S. Collins and R. Rodrigo, *J. Chem. Soc.*, *Perkin Trans. 1*, 1991, 3047.

2 B. Witkop, *Heterocycles*, 1998, **57**, 563; C. Christophersen, *Acta Chem. Scand.*, *Ser. B*, 1985, **39**, 517.

3 (*a*) D. Crich, M. Bruncko, S. Natarajan, B. K. Teo and D. A. Tocher, *Tetrahedron*, 1995, **51**, 2215; (*b*) D. E. Zembower, J. A. Gilbert and M. M. Ames, *J. Med. Chem.*, 1993, **36**, 305; (*c*) M. Somei, T. Kawasaki, Y. Fukui, F. Yamada, T. Kobayashi, H. Aoyama and D. Shinmyo, *Heterocycles*, 1992, **34**, 1877; (*d*) R. S. Iyer, B. F. Coles, K. D. Raney, R. Thier, F. P. Guengerich and T. M. Harris, *J. Am. Chem. Soc.*, 1994, **16**, 1602; (*e*) E. R. Civitello and H. Rapoport, *J. Org. Chem.*, 1994, **59**, 3775; (*f*) J. Bujons, F. Sánchez-Baeza and A. Messeguer, *Tetrahedron*, 1994, **50**, 7597.

4 H. Ishibashi, N. Mita, N. Matsuba, T. Kubo, M. Nakanishi and M. Ikeda, *J. Chem. Soc.*, *Perkin Trans. 1*, 1992, 2821.

5 M. S. Morales-Ríos, C. García-Martínez, M. A. Bucio and P. Joseph-Nathan, *Monatsh. Chem.*, 1996, **127**, 691.

6 M. S. Morales-Ríos, O. R. Suárez-Castillo, C. García-Martínez and P. Joseph-Nathan, *Synthesis*, 1998, 1755.

7 P. Y. Sollenberger and R. B. Martin, *J. Am. Chem. Soc.*, 1970, **92**, 4261.

8 M. S. Morales-Ríos and P. Joseph-Nathan, *Magn. Reson. Chem.*, 1987, **25**, 911.

9 E. M. Arnett, S. G. Maroldo, S. L. Schilling and J. A. Harrelson, *J. Am. Chem. Soc.*, 1984, **106**, 6759.

10 C. Cox and T. Lectka, *J. Org. Chem.*, 1998, **63**, 2426.

11 D. Buttar, M. H. Charlton, R. Docherty and J. Starbuck, *J. Chem. Soc.*, *Perkin Trans. 2*, 1998, 763.

12 K. B. Wiberg and K. E. Laidig, *J. Am. Chem. Soc.*, 1988, **110**, 1872.

13 O. R. Suárez-Castillo, M. García-Velgara, M. S. Morales-Ríos and P. Joseph-Nathan, *Can. J. Chem.*, 1997, **75**, 959.

14 M. Clark, R. D. Cramer III and N. Van Opdensch, *J. Comput. Chem.*, 1989, **10**, 982.

15 M. J. S. Dewar, E. G. Zoebisch, E. F. Healy and J. J. P. Stewart, *J. Am. Chem. Soc.*, 1985, **107**, 3902.

16 See, *e.g.*, W. J. Hehre, L. Radom, P. v. R. Schleyer and J. A. Pople, *Ab Initio Molecular Orbital Theory*, Wiley, New York, 1986.

17 PC Spartan plus, version 1.5, Wavefunction, Inc., Irvine, CA, 1998.

18 G. M. Sheldrick, SHELXS 86, in *Crystallographic Computing 3*, eds. G. M. Sheldrick, C. Kreuger and R. Goddard, Oxford University Press, 1985, p. 175.

Paper a908104f